Supporting Information

Prediction of two-dimensional C_3N_2 semiconductors with outstanding stability, moderate band gaps, and high carrier mobility

Longhui Li,[a] Rui Tan,*[a] Yulou Ouyang,[a] Xiaolin Wei,[a] and Zhenkun Tang*[a]

[a] *Key Laboratory of Micro-nano Energy Materials and Application Technologies, University of Hunan Province & College of Physics and Electronics Engineering, Hengyang Normal University, Hengyang 421002, China.*

E-mail: rtan@hynu.edu.cn, zktang@hynu.edu.cn

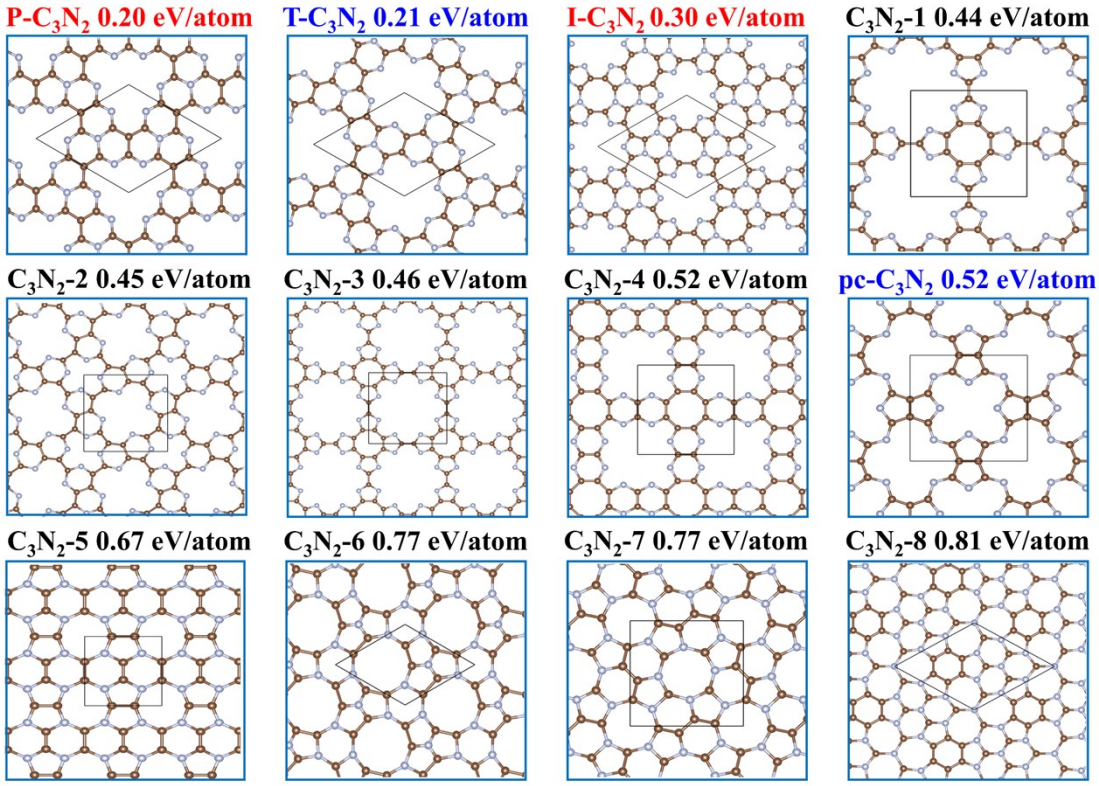

Fig. S1 The 12 reasonable C_3N_2 structures predicted by the RG^2 code, along with their calculated formation energies.

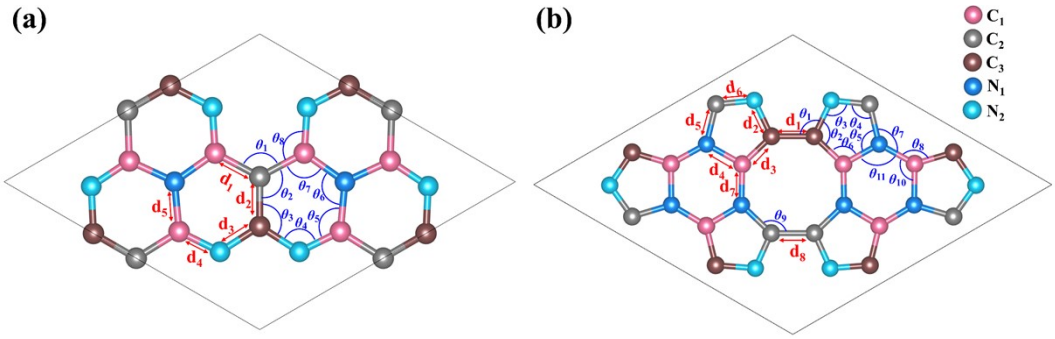

Fig. S2 The unit cells of (a) P-C_3N_2 and (b) I-C_3N_2 monolayers with inequivalent C and N atoms.

Table S1 The bond lengths and bond angles of P-C_3N_2.

Material	Bonds	Bond lengths (Å)	Bond angles	Angles (°)
P-C_3N_2	d_1	1.45	θ_1	123.9
	d_2	1.41	θ_2	118.1
	d_3	1.35	θ_3	122.7
	d_4	1.31	θ_4	121
	d_5	1.43	θ_5	121.5
			θ_6	120
			θ_7	116.7
			θ_8	121.8

Table S2 The bond lengths and bond angles of I-C_3N_2.

Material	Bonds	Bond lengths (Å)	Bond angles	Angles (°)
I-C_3N_2	d_1	1.46	θ_1	115.7
	d_2	1.36	θ_2	107.9
	d_3	1.39	θ_3	110.1
	d_4	1.41	θ_4	109.1
	d_5	1.41	θ_5	105.8
	d_6	1.32	θ_6	107.1
	d_7	1.39	θ_7	132.5
	d_8	1.48	θ_8	134.6
			θ_9	136.5
			θ_{10}	118.3
			θ_{11}	121.7

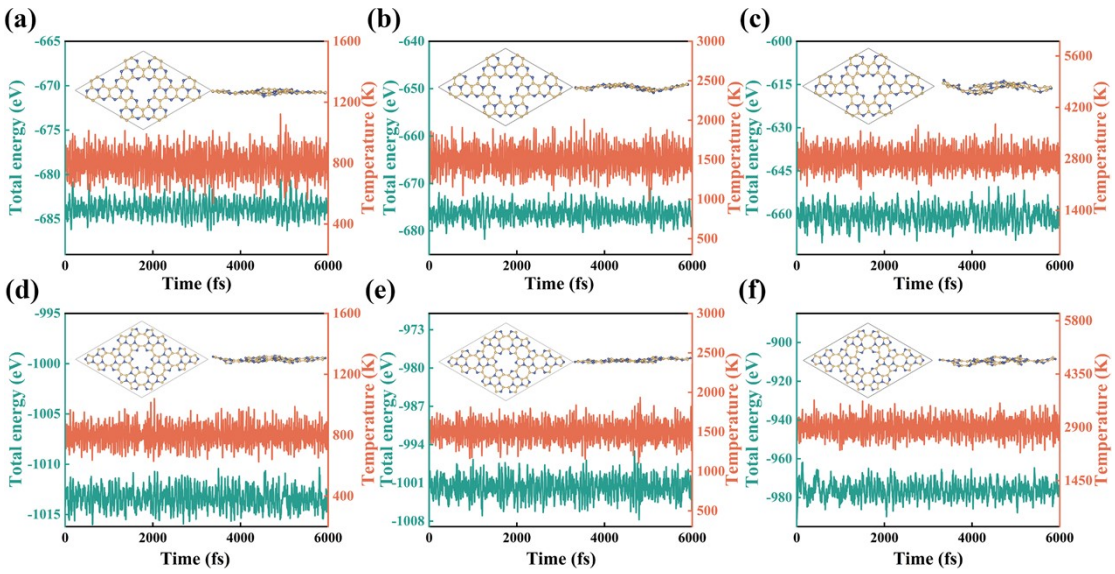

Fig. S3 (a-c) AIMD simulations of a 2 × 2 P-C_3N_2 supercell at 800,1500 and 2800 K. (d-f) AIMD simulations of a 2 × 2 I-C_3N_2 supercell at 800,1500 and 2900 K.

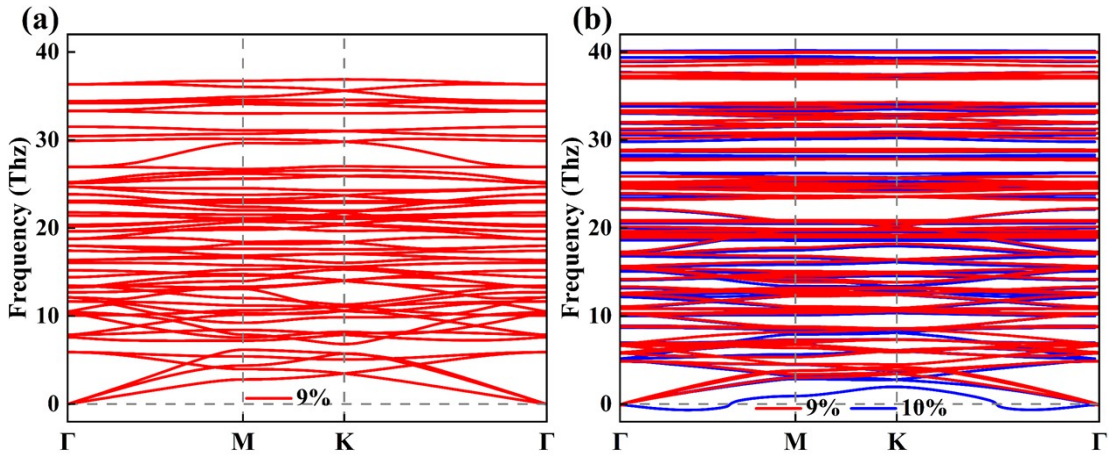

Fig. S4 (a) Phonon spectrum of P-C_3N_2 under 9% biaxial ultimate strain. (b) Phonon spectra of I-C_3N_2 under 9% and 10% biaxial strain.

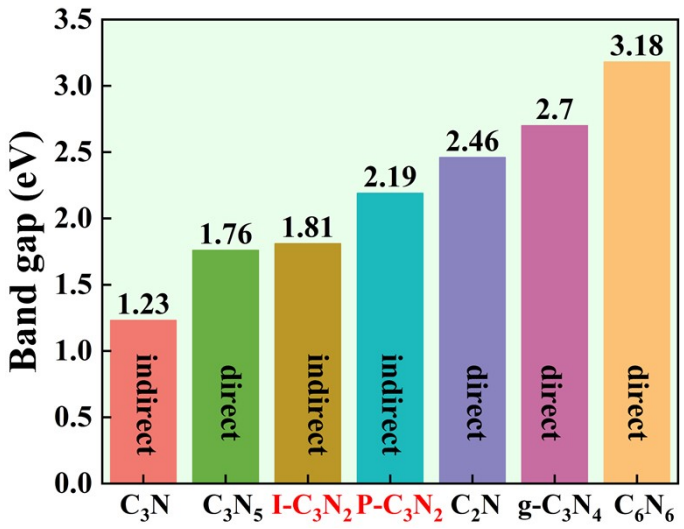

Fig. S5 Comparison of band gaps between two C_3N_2 monolayers and synthesized 2D carbon nitride materials.

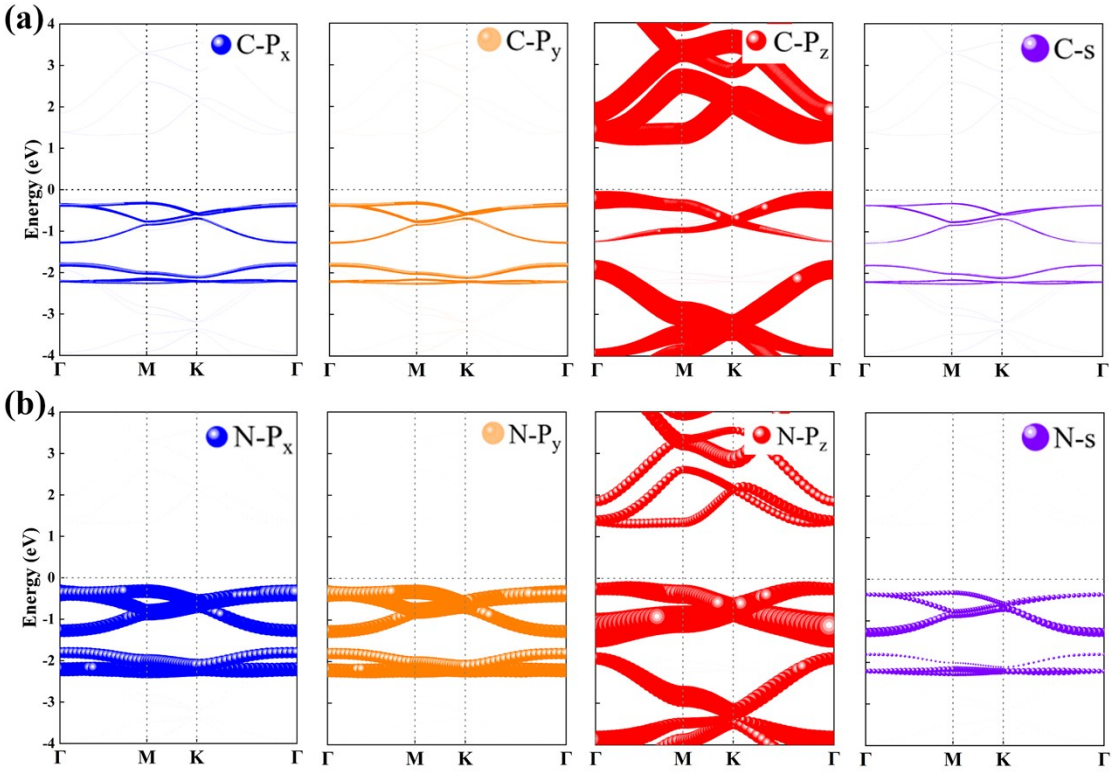

Fig. S6 The orbital-projected band structure of the P-C_3N_2 monolayer.

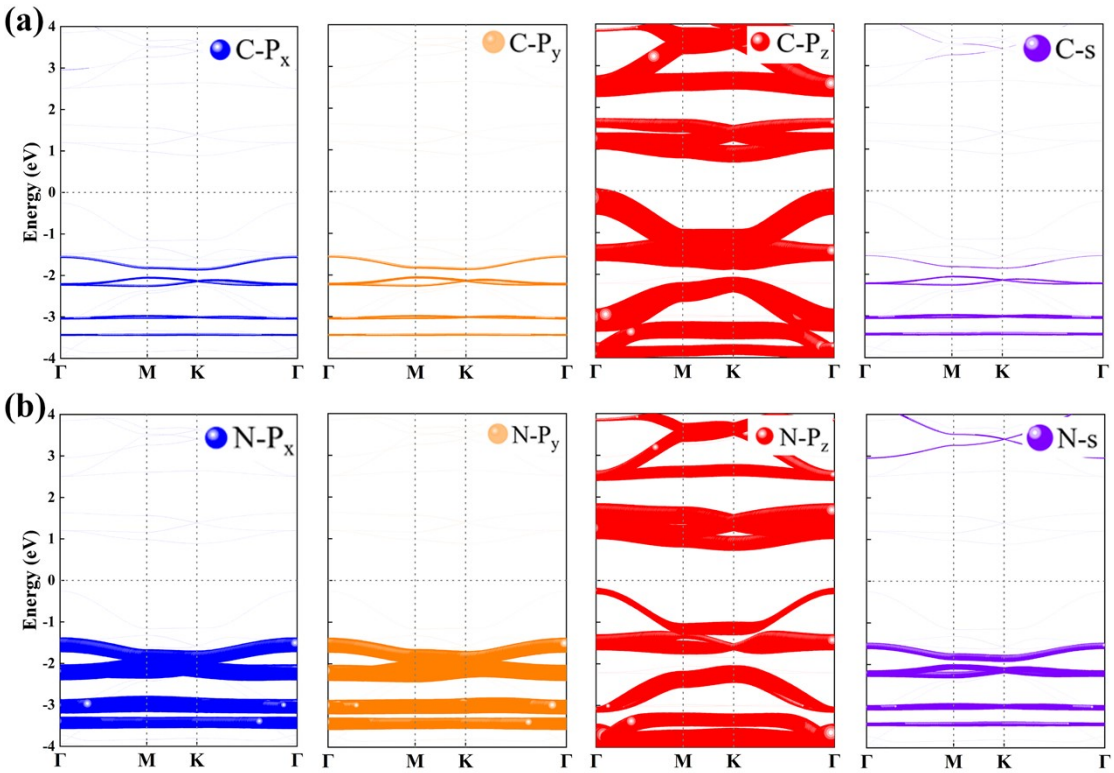

Fig. S7 The orbital-projected band structure of the I-C_3N_2 monolayer.

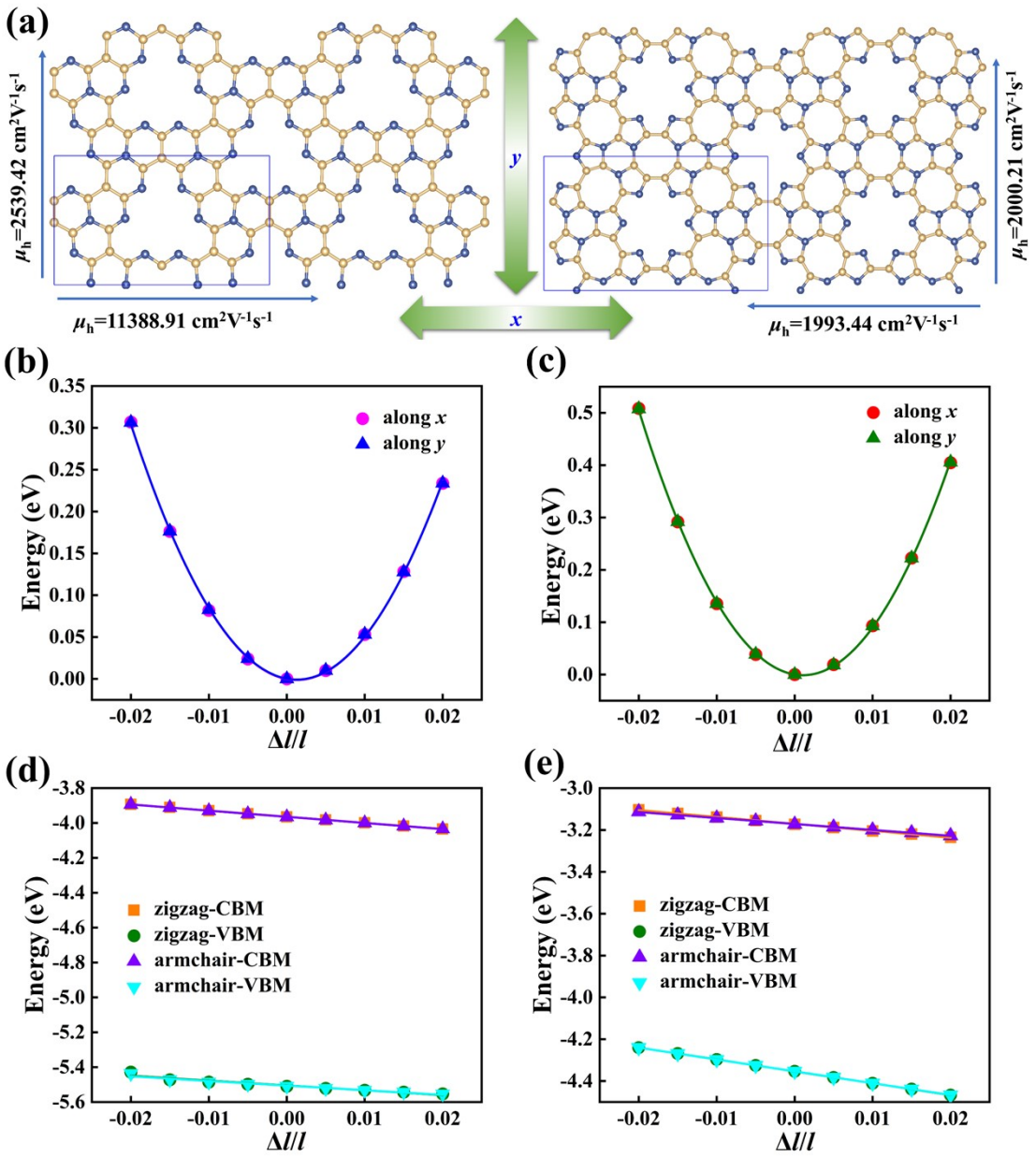

Fig. S8 (a) The orthorhombic structures and hole mobilities of the P-C_3N_2 and I-C_3N_2 along the *x* and *y* directions. (b)-(c) Total energy shift E-E_0 on the per surface as a function of lattice deformation $\Delta l/l$ along the *x* and *y* directions in P-C_3N_2 and I-C_3N_2. (d)-(e) Relationship between energy shift of the band edge position and the dilation $\Delta l/l$.

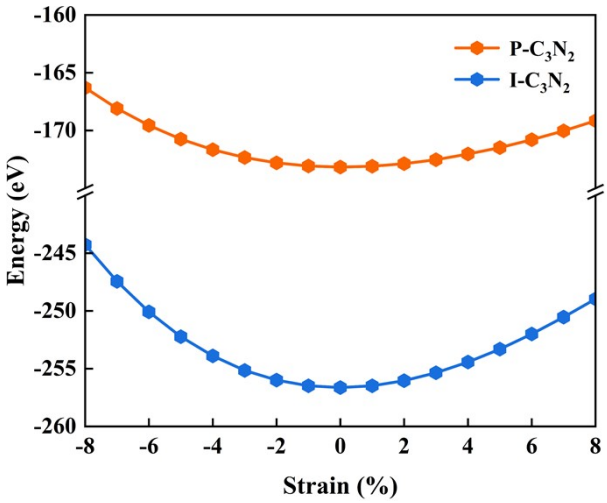

Fig. S9 Energy-strain curves of C_3N_2 monolayers under tensile and compression strains.

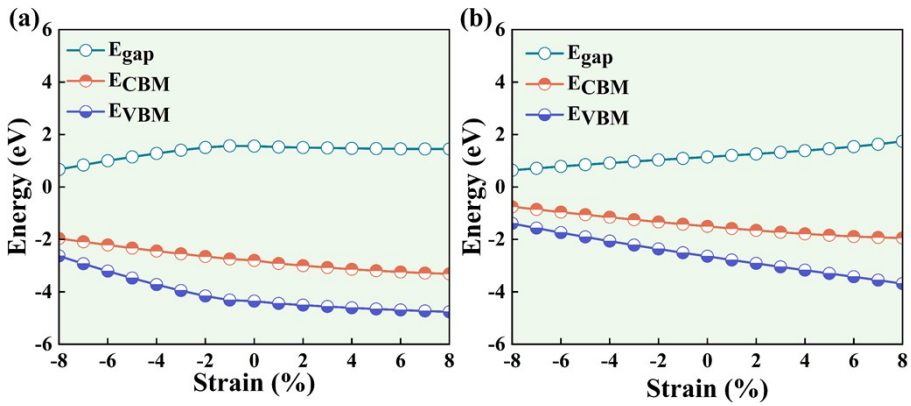

Fig. S10 Variations of energy eigen values of the CBM and VBM and band gap as functions of the biaxial strain of (a) P-C_3N_2 and (b) I-C_3N_2.

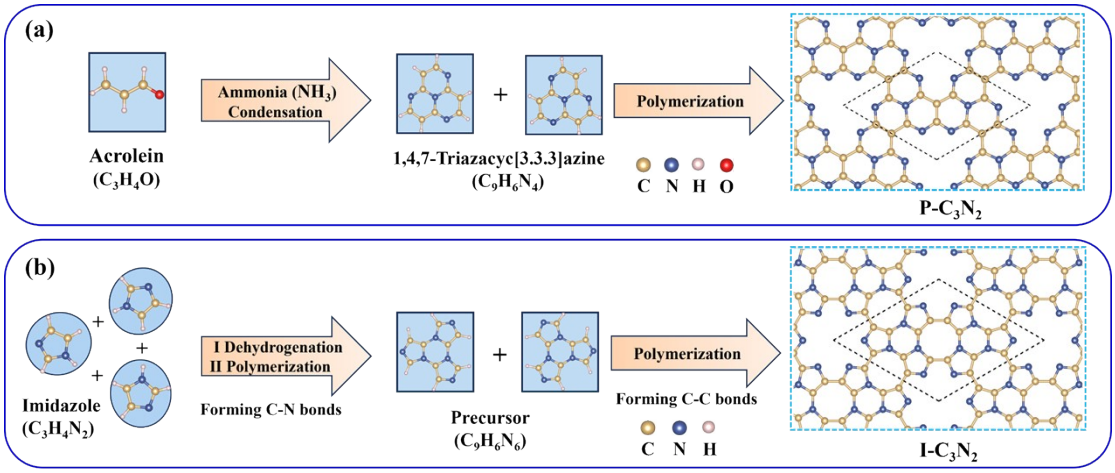

Fig. S11 The schematic synthesis process of (a) P-C_3N_2 and (b) I-C_3N_2.